Simple visco-elastic and visco-elasto-plastic models for geotechnical engineers

Author: Prof. Dr. habil. Heinz Konietzky
(TU Bergakademie Freiberg, Geotechnical Institute)

Editor: Prof. Dr.-Ing. habil. Heinz Konietzky Layout: Gunther Lüttschwager
TU Bergakademie Freiberg, Institut für Geotechnik, Gustav-Zeuner-Straße 1, 09599 Freiberg • sekr_fm@ifgt.tu-freiberg.de

1 Introduction

Rocks show time-dependent deformations under load (= creep) or stress relaxation under constant deformation (= relaxation).

The parameter viscosity [unit: Pa·s] is often used to quantify the time-dedendent behavior. Depending on type of geomaterial the viscosity can get values between about 10^{12} – 10^{22} Pa·s. For hard rocks values of about 10^{18} to 10^{20} Pa·s are typical. Please note, that creep behaviour is strongly dependent on temperature, pressure and water content.

Time-dependent behaviour, for instance visco-elastic or visco-elasto-plastic behaviour, can be described in different ways. One popular and intuitive way is the use of rheological basic elements. By interconnection of several of such basic elements in series or in parallel complex and non-linear time-dependent material behavior can be simulated.

This ebook provides an introduction into the most popular basic rheological elements and their interconnection to describe time-dependent behavior of geomaterials as exemplary shown in Fig. 1.1 for a rock specimen under uniaxial constant loading. Depending on the use and interconnection of basic rheological elements some or all of the creep phases can be simulated.

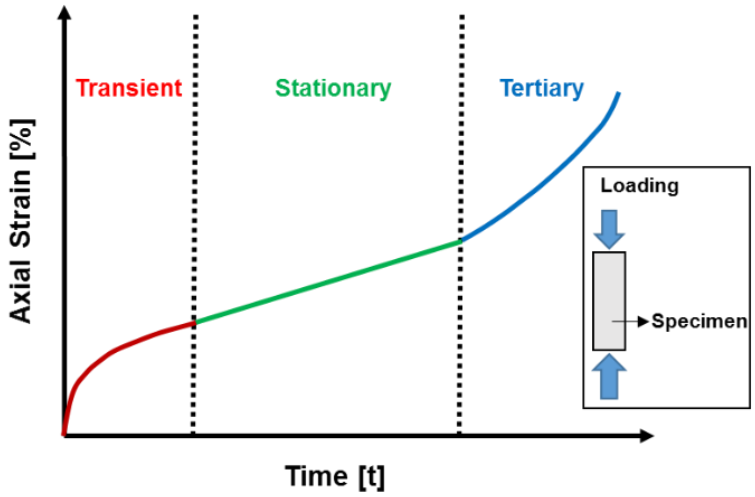

Fig. 1.1: Creep curve typical for rocks with three phases: primary (transient), secondary (stationary) and tertiary (failure) creep

Tsugawa et al. (2019) provide a more general overview about the rheology for soils and rocks incl. determination of parameters and applications in geotechnical engineering.

2 Basic rheological elements

Visco-elastic and visco-elasto-plastic models can be composed by several basic elements. The most popular are:

- Dashpot

- Spring

- Slider (St. Venant Element)

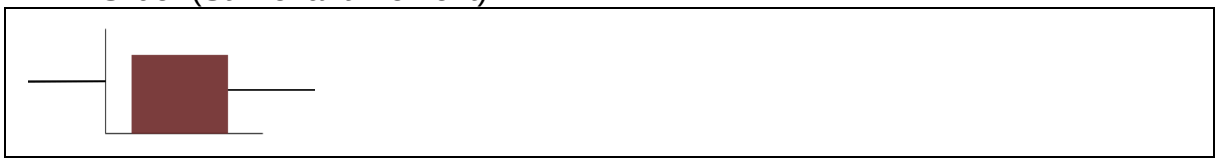

The equations for these basic elements (1-dimensional) are as follows:

- For spring (elastic):

$$\sigma = E \cdot \varepsilon$$

- For slider (St. Venant element; plastic)

$$\varepsilon = \begin{cases} 0 \quad for \quad \sigma < \sigma_f \\ \varepsilon(t) \quad for \quad \sigma \geq \sigma_f \end{cases}$$

- For dashpot (viscous):

$$\sigma = \eta \cdot \dot{\varepsilon}$$

where:

σ = stress, ε = deformation, η = viscosity, t = time, σ_f = failure (limit) stress, E = Young's modulus

Fig. 2.1 illustrates the behaviour of the above mentioned three basis reheological elements.

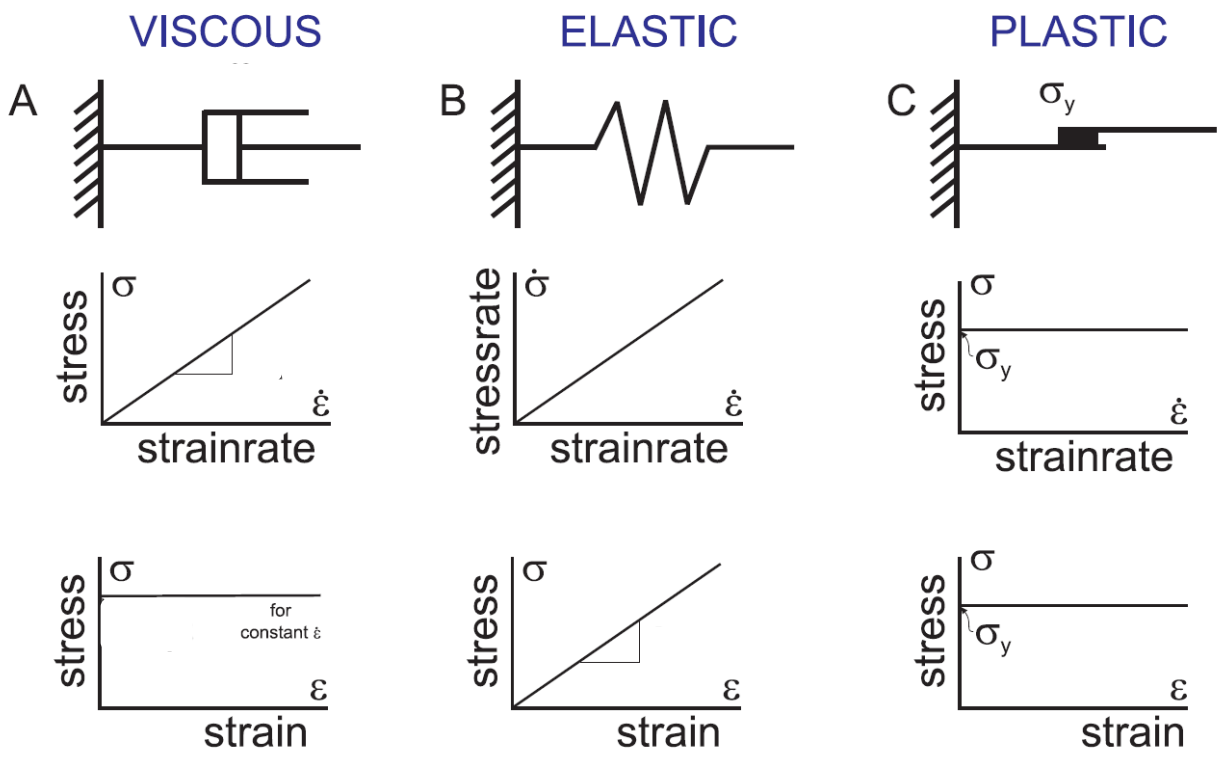

Fig. 2.1: Behaviour of rheological basic elements

3 Visco-elastic models

Within this chapter the most popular visco-elastic models are presented, which consist of interconnections of springs and dashpots.

3.1 Maxwell model

The Maxwell model consists of a spring and a dashpot in series like shown in Fig. 3.1.1. The corresponding differential equations reads as follows:

$$\dot{\varepsilon} = \frac{\sigma}{\eta_M} + \frac{\dot{\sigma}}{E_M}$$

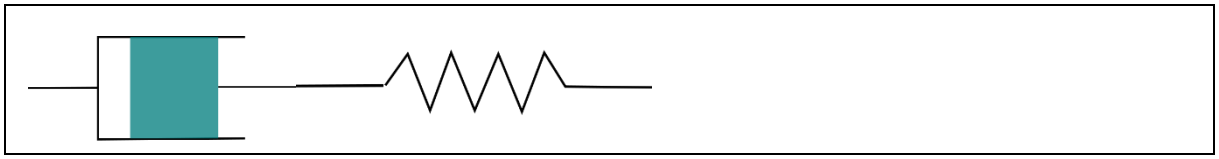

Fig. 3.1.1: Maxwell model

3.2 Kelvin model

The Kelvin model consists of a spring and a dashpot interconnected parallel like shown in Fig. 3.1.2. The corresponding differential equations reads as follows:

$$\sigma = E_K \cdot \varepsilon + \eta_K \cdot \dot{\varepsilon}$$

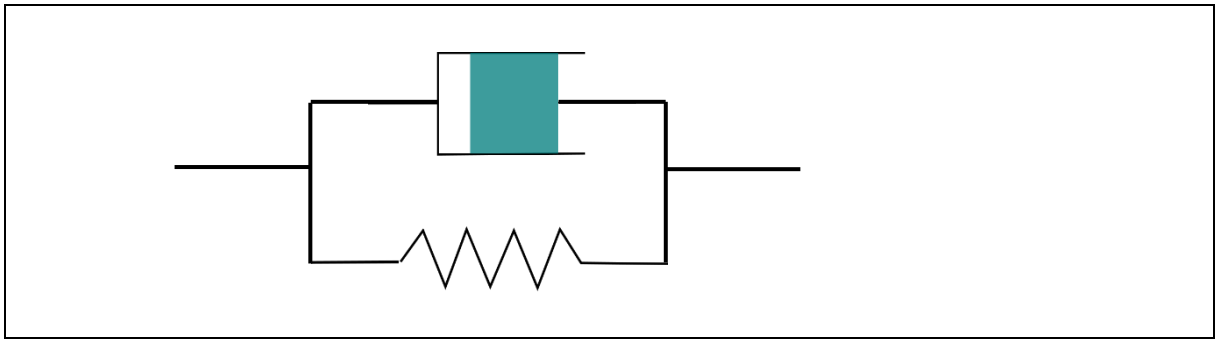

Fig. 3.1.2: Kelvin model

3.3 Burgers model

The Burgers model consists of the Kelvin model in series with the Maxwell model like shown in Fig. 3.3.1. The corresponding differential equations reads as follows:

$$\dot{\varepsilon}\cdot\eta_M+\ddot{\varepsilon}\cdot\frac{\eta_M\eta_K}{E_K}=\sigma+\dot{\sigma}\cdot\left(\frac{\eta_M}{E_M}+\frac{\eta_K}{E_K}+\frac{\eta_M}{E_K}\right)+\ddot{\sigma}\frac{\eta_M\eta_K}{E_ME_K}$$

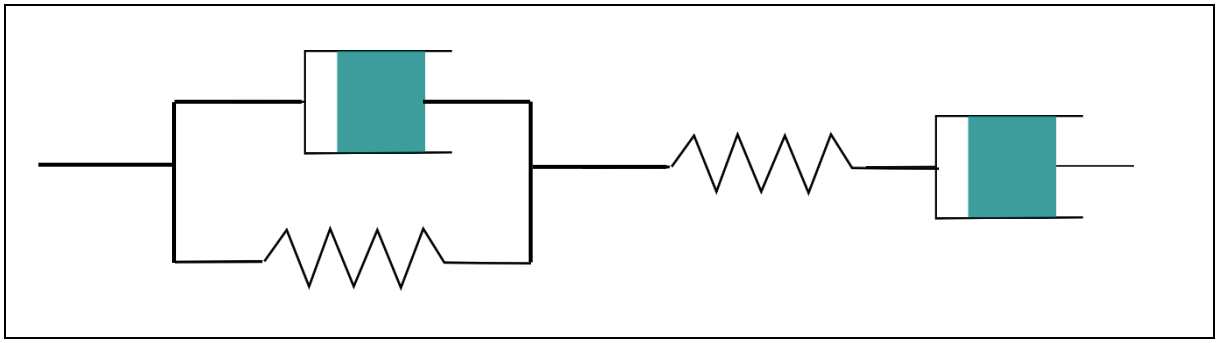

Fig. 3.3.1: Burgers model

3.4 Extended Kelvin Model I

The extended Kelvin model I consists of the Kelvin model with an additional spring in series like shown in Fig. 3.4.1. The corresponding differential equations reads as follows:

$$\sigma\cdot(E_M+E_K)+\dot{\sigma}\cdot\eta_K=E_M\cdot E_K\cdot\varepsilon+E_{eK}\cdot\eta_K\cdot\varepsilon$$

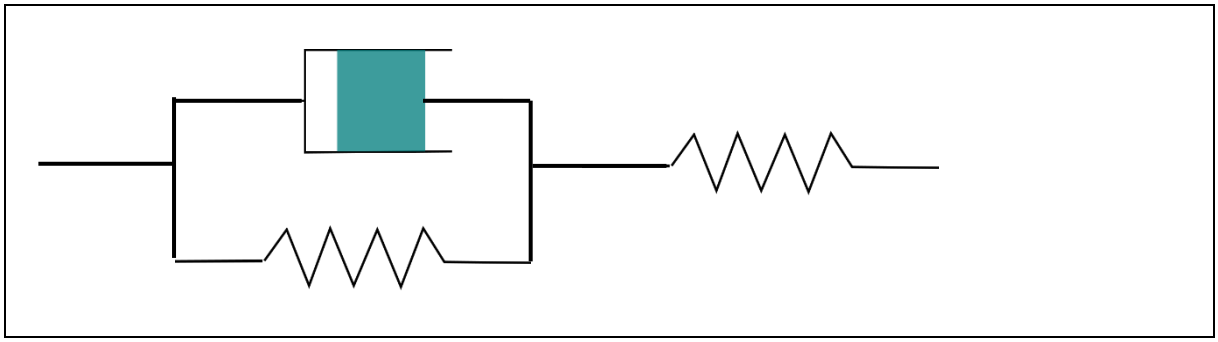

Fig. 3.4.1: Extended Kelvin model I

3.5 Extended Kelvin Model II

The extended Kelvin model II consists of the Kelvin model with an additional dashpot in series like shown in Fig. 3.5.1. The corresponding differential equations reads as follows:

$$\sigma \cdot E + (\eta_K + \eta_{eK}) \cdot \dot{\sigma} = E \cdot \eta_{eK} \cdot \dot{\varepsilon} + \eta_K \cdot \eta_{eK} \cdot \ddot{\varepsilon}$$

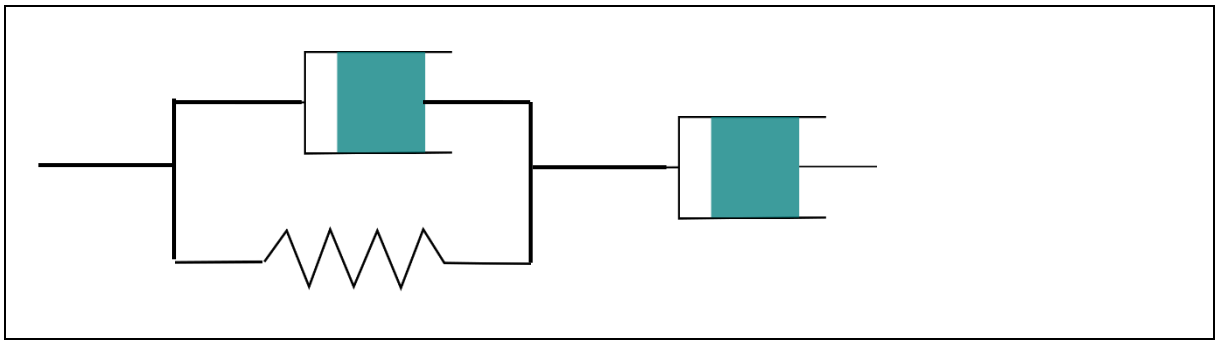

Fig. 3.5.1: Extended Kelvin model II

3.6 Zener Model

The Zener model is based on the Kelvin model, but with an additional spring in series with the dashpot like shown in Fig. 3.6.1. The corresponding differential equations reads as follows:

$$\frac{\sigma}{E_K \eta_K} + \frac{\dot{\sigma}}{E_K E_Z} = \frac{\varepsilon}{\eta_K} + \frac{\dot{\varepsilon} \cdot (E_K + E_Z)}{E_K E_Z}$$

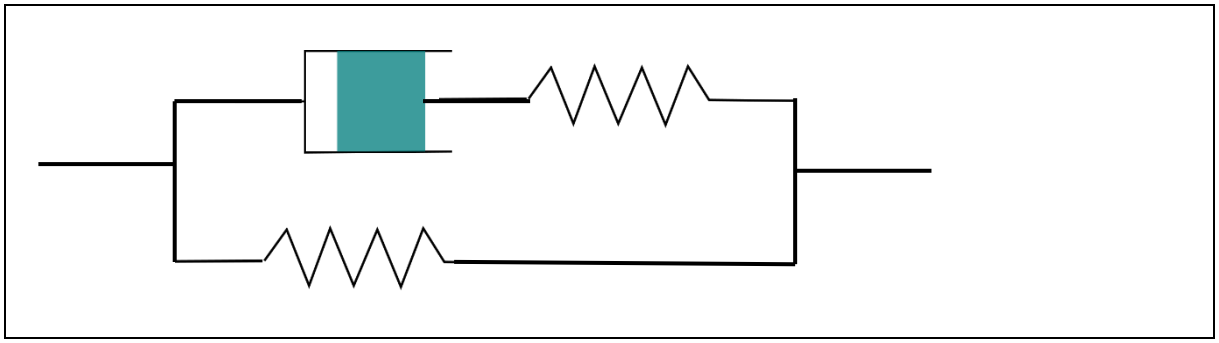

Fig. 3.6.1: Zener model

3.7 Extended Maxwell model

The extended Maxwell model is based on the Maxwell model extended by an additional dashpot acting in parallel like shown in Fig. 3.7.1. The corresponding differential equations reads as follows:

$$\sigma \cdot E + \eta_M \cdot \dot{\sigma} = (\eta_M + \eta_{eM}) \cdot E \cdot \dot{\varepsilon} + \eta_M \cdot \eta_{eM} \cdot \ddot{\varepsilon}$$

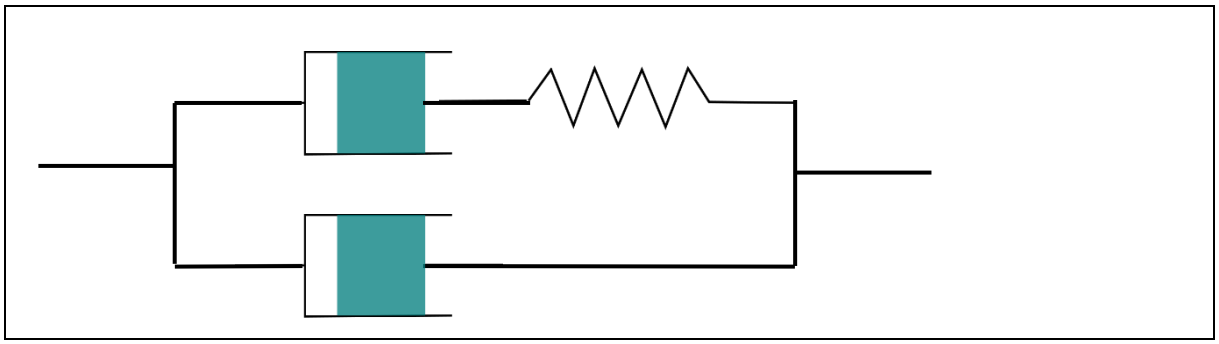

Fig. 3.7.1: Extended Maxwell model

3.8 Generalized visco-elastic models

Linear visco-elastic models like given above can be generalized as follows:

$$F_1 \cdot \sigma + F_2 \cdot \dot{\sigma} + F_3 \cdot \ddot{\sigma} + F_4 \cdot \dddot{\sigma} + \ldots = f_1 \cdot \varepsilon + f_2 \cdot \dot{\varepsilon} + f_3 \cdot \ddot{\varepsilon} + f_4 \cdot \dddot{\varepsilon} + \ldots$$

where: F_1 etc. and f_1 etc. are material properties or functions. The more elements are included, the higher the degree of the differential equations.

Non-linearity can be achieved if stress is proportional to any power n of deformation, for instance:

$\sigma = E \cdot \varepsilon^n$ for a non-linear spring

$\sigma = \varepsilon^n \cdot \dot{\varepsilon}$ for a non-linear dashpot

4 Visco-elasto-plastic models

4.1 Bingham model

In the Bingham model a dashpot and a St. Venant element act in parallel like shown in Fig. 4.1.1. This is a pure visco-plastic model. The corresponding differential equations reads as follows:

$$\begin{aligned} \sigma &= \sigma_0 + \eta \cdot \dot{\varepsilon} \\ \dot{\varepsilon} &= 0 \end{aligned} \quad \text{for} \quad \begin{aligned} \sigma &> \sigma_f \\ \sigma &< \sigma_f \end{aligned}$$

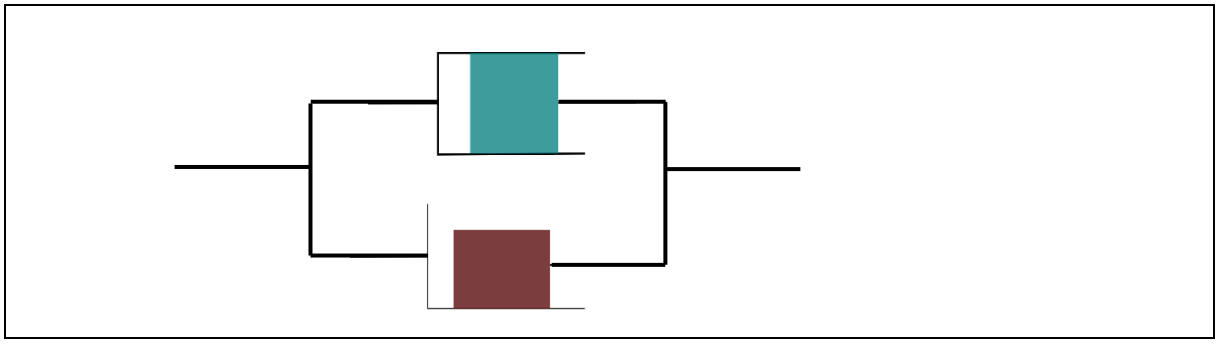

Fig. 4.1.1: Bingham model

4.2 Loonen model

The Loonen model can be considered as an extension of the Bingham model by integrating an additional spring, which makes this model to a simple visco-elasto-plastic model. The corresponding differential equations reads as follows:

$$\begin{aligned} \sigma &= \sigma_0 + \eta \cdot \dot{\varepsilon} \\ \sigma &= E \cdot \varepsilon + \eta \cdot \dot{\varepsilon} \end{aligned} \quad \text{for} \quad \begin{aligned} \sigma &> \sigma_f \\ \sigma &< \sigma_f \end{aligned}$$

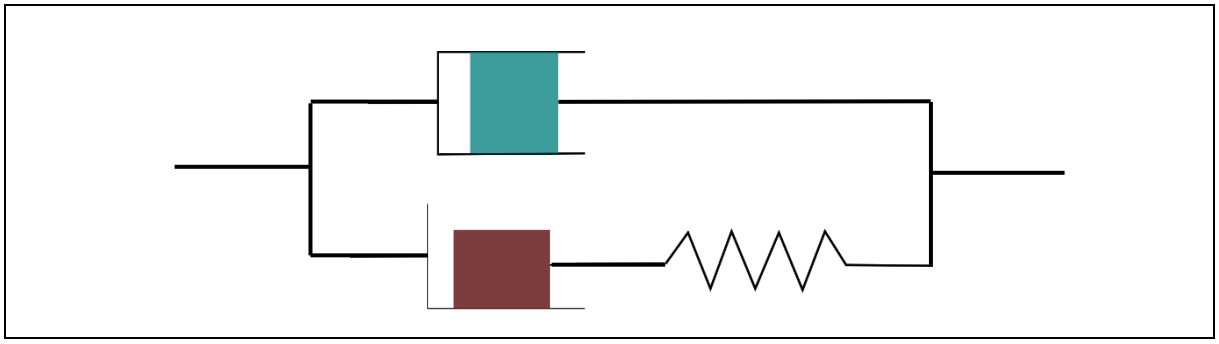

Fig. 4.2.1: Loonen model

4.3 Comparison of different models

Tarifard et al. (2024) provide an excellent overview about creep constitutive models covering pure empirical models based on fitting functions, but focus on analytical models based on rheological elements. The most popular ones are illustrated in Fig. 4.3.1.

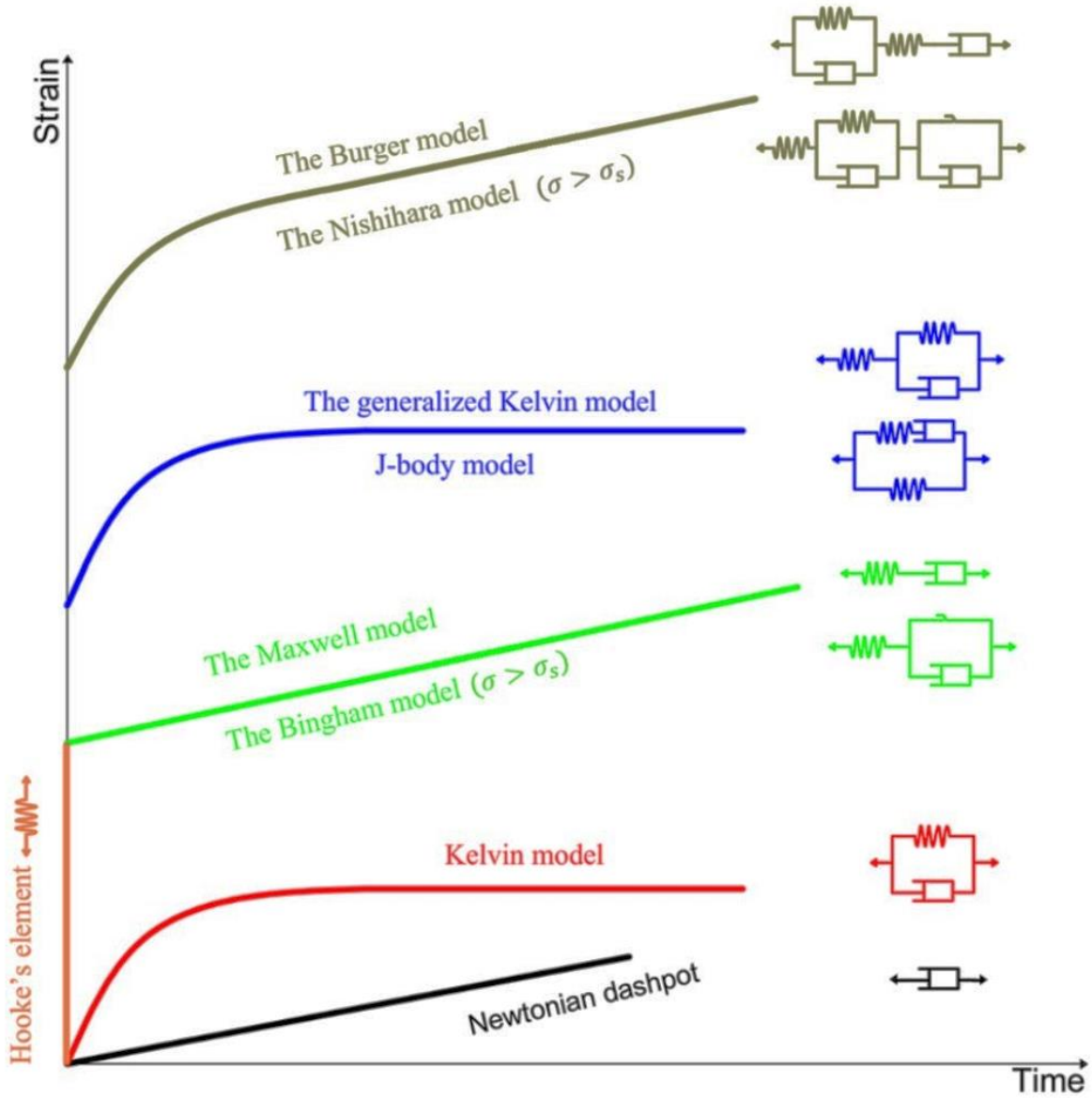

Fig. 4.3.1: General creep curves of several creep models popular in geomechanics (Tarifard et al., 2024)

5 Creep and relaxation

The above listed models are described by linear differential equations. The corresponding stress-strain relations can be obtained analytically or numerically. Two special constellations are of major interest:

Creep: load is constant ($\sigma = \sigma_0 = const.$) and deformation develops over time

Relaxation: deformation is constant ($\varepsilon = \varepsilon_0 = const.$) and stress relaxation develops over time

The mathematical expressions and the corresponding σ-t- and ε-t-diagrams for some selected models are given below (see also Fig. 5.1 to 5.3):

Maxwell model:

Creep: $\varepsilon = \frac{\sigma_0}{\eta} \cdot t + \frac{\sigma_0}{E}$ Relaxation: $\sigma = \sigma_0 \cdot e^{\frac{t \cdot E}{\eta}}$

Kelvin model:

Creep: $\varepsilon = \frac{\sigma_0}{E} \cdot \left(1 - e^{\frac{t \cdot E}{\eta}}\right)$ Relaxation: $\sigma = const.$

Burgers model:

Creep: $\varepsilon = \frac{\sigma_0}{E_M} + \frac{\sigma_0}{\eta_M} \cdot t + \frac{\sigma_0}{E_K} \cdot \left(1 - e^{\frac{t \cdot E_K}{\eta_K}}\right)$

Relaxation: $\sigma = \frac{\sigma_0}{K_1 - K_2} \left[(K_1 - 1) \cdot e^{-K_1 \frac{tE_K}{\eta_K}} - (K_2 - 1) \cdot e^{-K_2 \frac{tE_K}{\eta_K}} \right]$

with: $K_{1/2} = \frac{1}{2}\left(1 + \frac{E_M}{E_K} + \frac{\eta_K E_M}{\eta_M E_K}\right) \pm \sqrt{\left[\left(1 + \frac{\eta_K E_M}{\eta_M E_K} + \frac{E_M}{E_K} 4\right)^2 - 4 \cdot \frac{\eta_K E_M}{\eta_M E_K}\right]}$

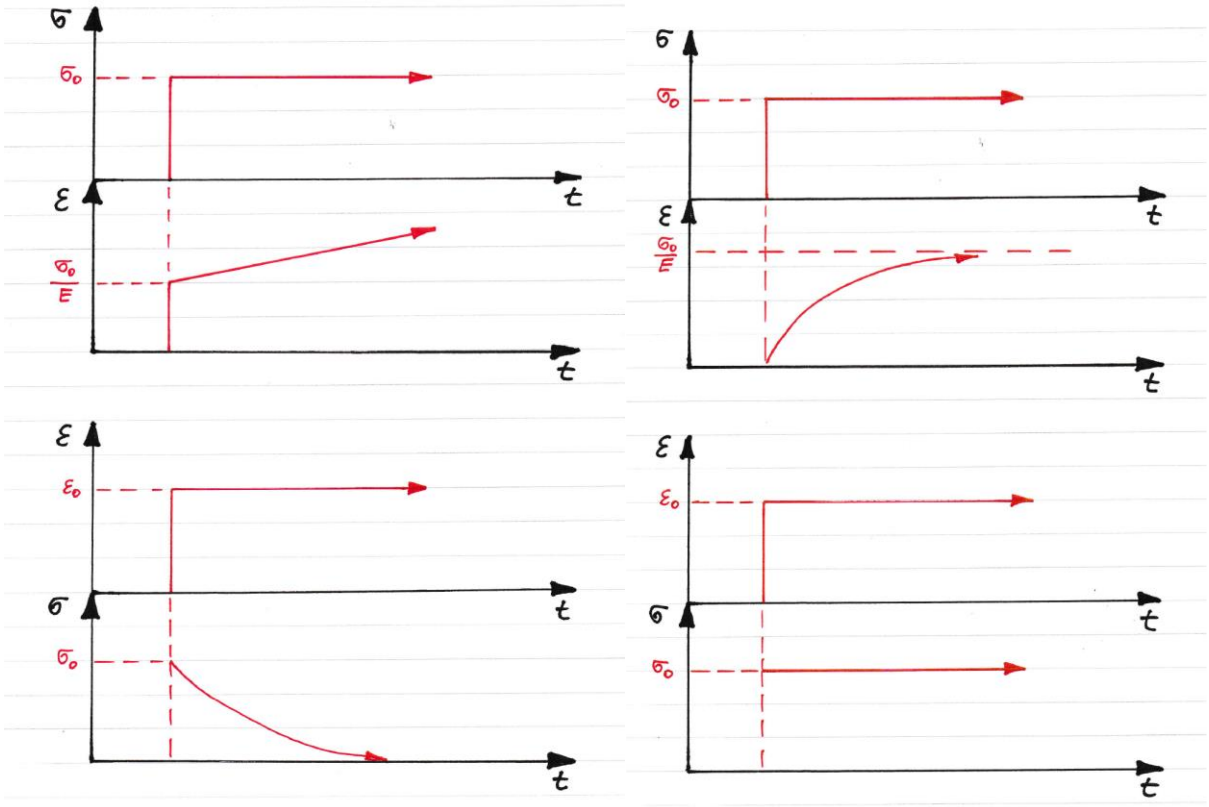

Fig. 5.1: Creep and relaxation curves for Maxwell (left) and Kelvin (right) models

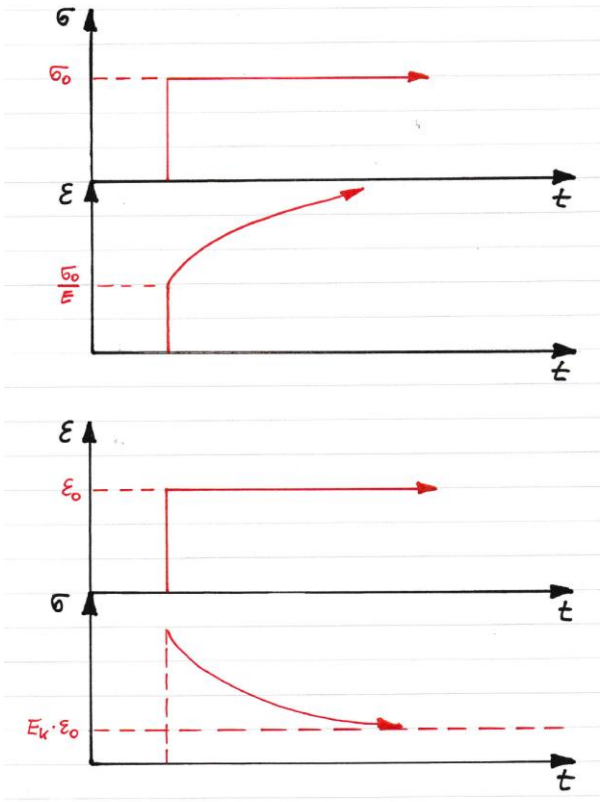

Fig. 5.2: Creep and relaxation curves for Burgers model

Fig. 5.1 and 5.2 show the creep (σ_0 = const.) and relaxation (ε_0 = const.) curves for the Maxwell, Kelvin and Burgers models. Please note, that during creep of the Burgers model the deformation is composed first of the instantaneous reaction of the Maxwell model (pure elastic response) followed by the superposiion of the linearly rising Maxwell strain and the non-linear rising Kelvin strain.

Fig. 5.3 illustrates the deformation-time curve for the Burgers model for loading followed by unloading.

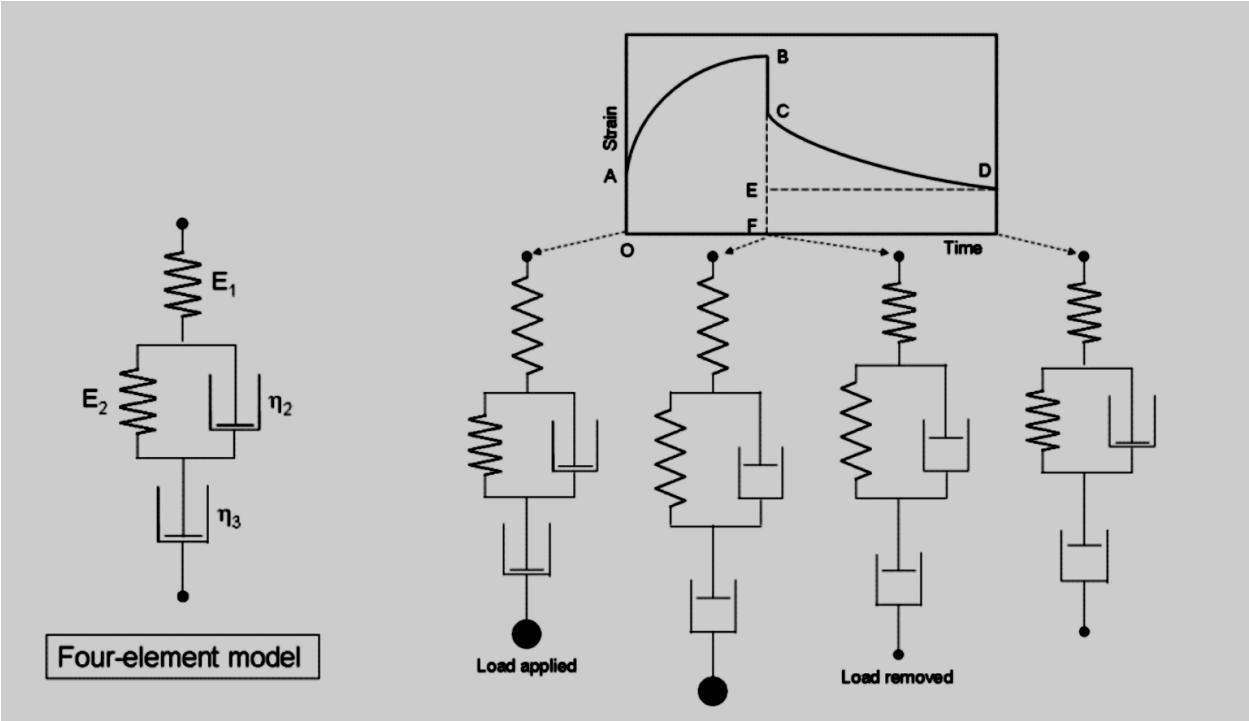

Fig. 5.3: Deformation behavior of Burgers model (loading and unloading) (Murata, 2012)

A more comprehensive model for rocks considering also plasticity was proposed by Wu et al. (2013). This model is able to describe primary, secondary and tertiary creep, like shown in Fig. 5.4. The creep deformation is given by the following equation (see also Fig. 5.4 and 5.5; n is specific creep constant):

$$\varepsilon = \left[\frac{1}{G_1} + \frac{1}{G_2}\left(1 - e^{-\frac{G_2 t}{\eta_1}}\right) + \frac{1}{G_3}\left(1 - e^{-\frac{G_3 t}{\eta_2}}\right)\right] \cdot \sigma_0 + \frac{H(\sigma_0 - \sigma_s)}{\eta_3} \cdot \left[e^{t^n} - 1\right]$$

where: $$H(\sigma_0 - \sigma_S) = \begin{cases} 0 \;\; for \;\; \sigma_0 \le \sigma_S \\ \sigma_0 - \sigma_S \;\; for \;\; \sigma_0 > \sigma_S \end{cases}$$

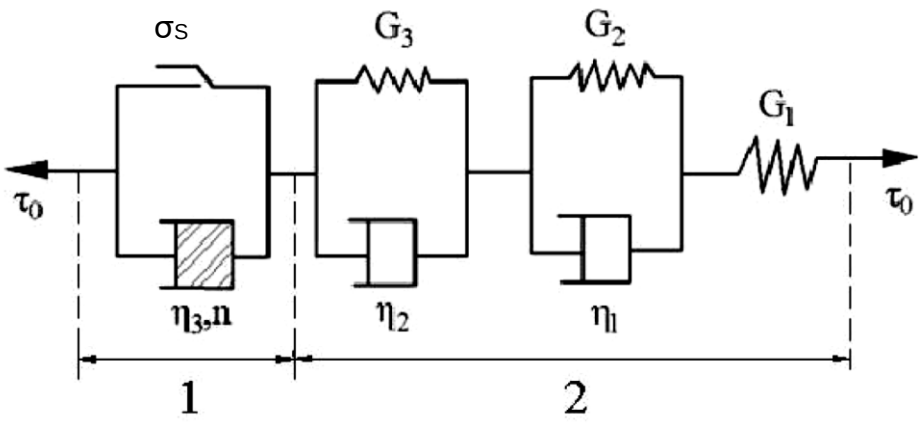

Fig. 5.4: Rheological model for creep simulation of rocks (Wu et al., 2013)

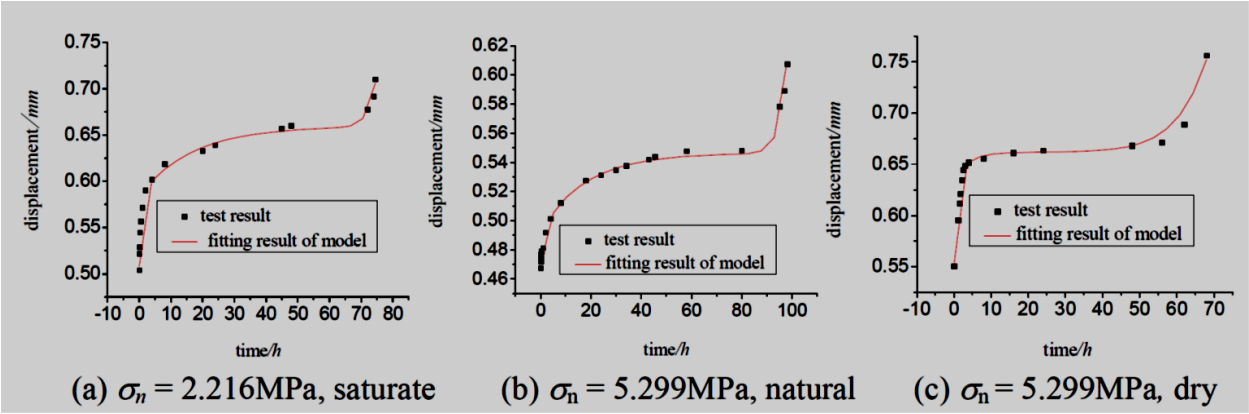

Fig. 5.5: Comparison between lab tests and rheological model according to Wu et al. (2013) for different creep load levels and water saturation conditions

6 Rockmechanical application

A creeping reservoir slope at the water reservoir Schoenbrunn in Germany was investigated and monitored in detail over a time span of more than 30 years. Finally a corresponding numerical model was set-up to predict the slope behavior (creep deformation and potential failure) under extreme precipitation szenarios. The applied numerical model is based on the elasto-plastic Burgers model extended by MC-plasticity and considering the water effect. Fig. 6.1 illustrates the applied constitutive model and Fig. 6.2 and 6.3 show the continuum and discontinuum models used to simulate the creep process using the rheological model according to Fig. 6.1. Exemplary, Fig. 6.4 shows the obtained time-dependent displacement evolution for different observation points at the slope surface.

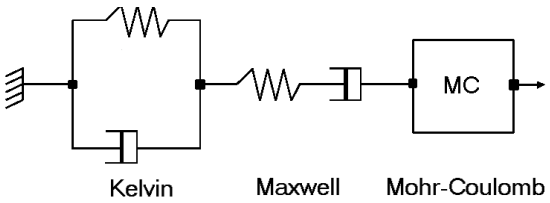

Fig. 6.1: Applied numerical model for backanalysis and predictions for creeping reservoir slope (Konietzky et al., 2004a)

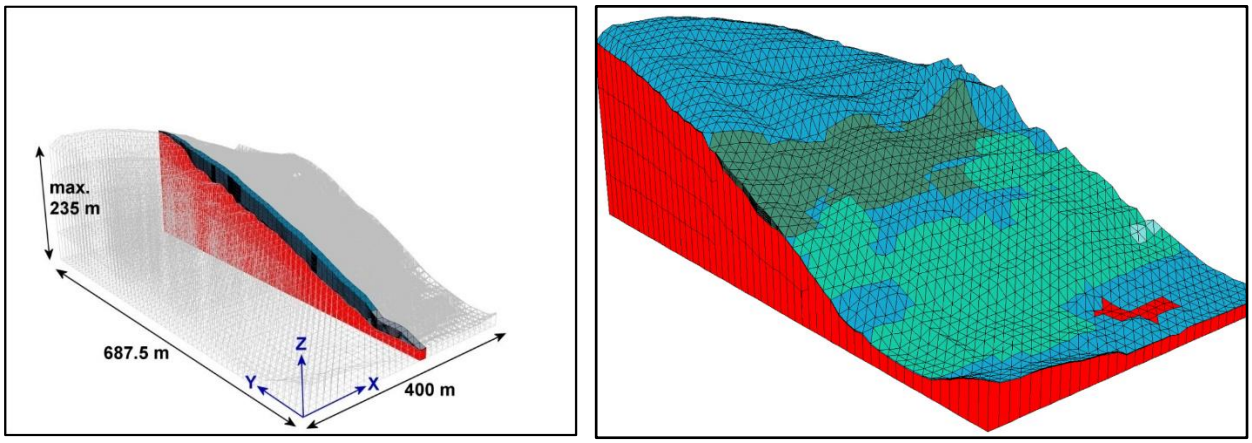

Fig. 6.1.2: Continuum mechanical model for backanalysis and predictions of creeping reservoir slope (Konietzky et al., 2004b)

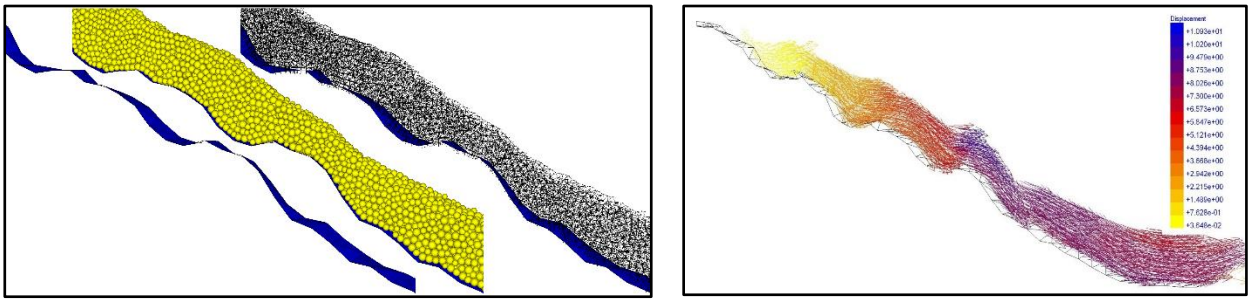

Fig. 6.1.3: Discontinuum mechanical model for backanalysis and predictions of creeping reservoir slope (Konietzky et al., 2004b)

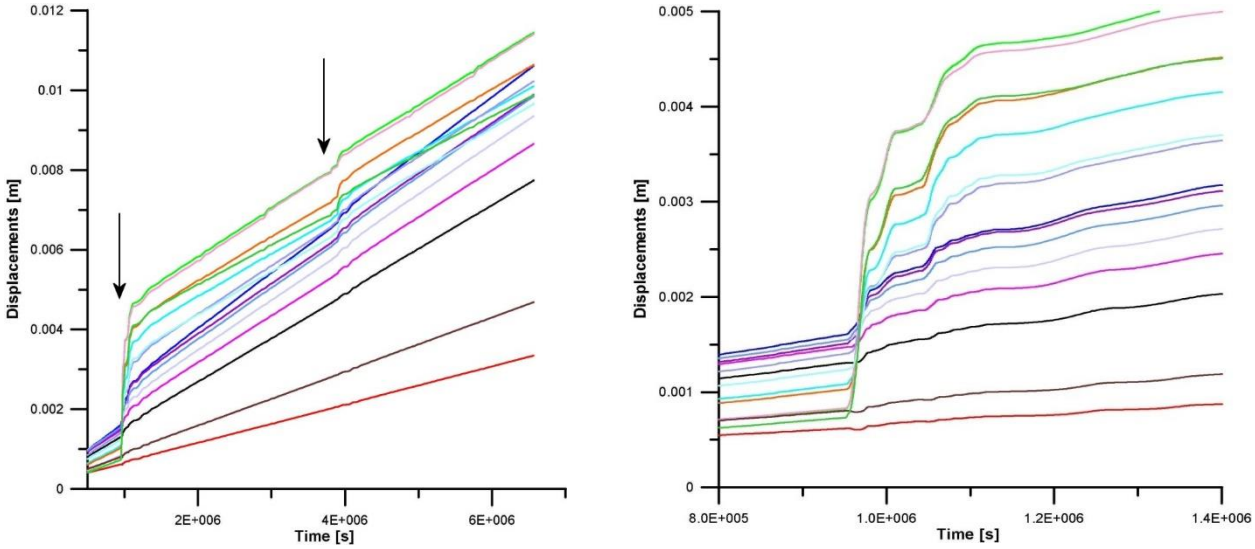

Fig. 6.1.4: Displacement evolution for selected observation points at the slope surface versus time (arrows indicate points in time with strong precipitation, which accelerate displacements as shown in the time-widow plot at the right hand site) (Konietzky et al., 2004b)

7 References

Konietzky H. et al. (2004a): Complex 3D landslide simulation. Proc. Landslides: evaluation and stabilization, Taylor & Francis, 1053–1059

Konietzky, H. et al. (2004b): Simulation of landslide movements based on a multidisciplinary approach, Felsbau, 22-2: 23-32.

Murata, H. (2012): Rheology – Theory and applications to biomaterials, DOI: 10.5772/48393

Tsugawa, J.K. et al. (2019): Review: rheology concepts applied to geotechnical engineering, Appl. Rheology, 29(1): 202-221

Tarifard, A. et al. (2024): Review of the creep constitutive models for rocks and the application of creep analysis in geomechanics, Rock Mech. Rock Eng., 57:7727-7757

Wu, L. et al. (2013): Study on the constitutive model of visco-elasticity-plasticity considering the rheology of rock mass, Advanced Materials Research, 639-640: 567-572